Proper division plane orientation and mitotic progression together allow normal growth of maize

Pablo Martinez[a,b], Anding Luo[c], Anne Sylvester[c], and Carolyn G. Rasmussen[a,1]

[a]Department of Botany and Plant Sciences, Center for Plant Cell Biology, University of California, Riverside, CA 92521; [b]Biochemistry and Molecular Biology Graduate Program, University of California, Riverside, CA 92521; and [c]Department of Molecular Biology, University of Wyoming, Laramie, WY 82071

Edited by Elliot M. Meyerowitz, Howard Hughes Medical Institute and California Institute of Technology, Pasadena, CA, and approved January 17, 2017 (received for review November 23, 2016)

How growth, microtubule dynamics, and cell-cycle progression are coordinated is one of the unsolved mysteries of cell biology. A maize mutant, *tangled1*, with known defects in growth and proper division plane orientation, and a recently characterized cell-cycle delay identified by time-lapse imaging, was used to clarify the relationship between growth, cell cycle, and proper division plane orientation. The *tangled1* mutant was fully rescued by introduction of cortical division site localized TANGLED1-YFP. A CYCLIN1B destruction box was fused to TANGLED1-YFP to generate a line that mostly rescued the division plane defect but still showed cell-cycle delays when expressed in the *tangled1* mutant. Although an intermediate growth phenotype between wild-type and the *tangled1* mutant was expected, these partially rescued plants grew as well as wild-type siblings, indicating that mitotic progression delays alone do not alter overall growth. These data indicate that division plane orientation, together with proper cell-cycle progression, is critical for plant growth.

maize | division | phragmoplast | TANGLED | cell cycle

Plant cells are surrounded by a cell wall that together with other cellular factors, controls cell growth and restricts cell movement. According to cell theory, the orientation of the division plane sets the ultimate placement of cells and is therefore key for the overall organization of the plant body. Alternately, according to organismal theory, cell partitioning merely fills in space, and therefore division plane orientation plays no role in overall plant organization (1). Multiple examples exist that support one theory or the other, but a combined theory whereby overall growth is regulated at the organ level, but executed by cells, may be the most accurate (2). Cell walls are positioned during the cell cycle with the involvement of characteristic microtubule arrays: a preprophase band (PPB), which assembles in late interphase (G2) and predicts the future division site (3); a spindle in metaphase and anaphase; and a phragmoplast during telophase and cytokinesis that directs the formation of the new cell wall to the cortical division site (4–6). The PPB is not required for cytokinesis but is critical for division plane orientation and may be required for timely cell-cycle progression (7, 8). The PPB disassembles before cytokinesis, raising the fundamental question of how the premitotic location of the PPB specifies the position of the future new wall (9).

Mutants with general division plane defects often have significant alterations in both microtubule organization and overall growth (10–12). Alternatively, mutants may have defective specific asymmetric divisions leading to developmental defects (13–19). Many mutants with general division plane defects have mutations in genes that encode microtubule-associated proteins that disrupt both mitotic and interphase microtubule dynamics. In these cases, it is difficult to separate the relative contribution of mitotic versus interphase functions in wall placement. The division plane mutant *tangled1* (*tan1*) is particularly informative because the TAN1 protein is observed only in mitotic cells (20, 21) and binds microtubules in vitro (22). Analysis of the *tan1* mutant is therefore used here to elucidate the specific contribution of microtubule dynamics during mitosis. Similar to mutants with defects in both interphase and mitotic microtubule dynamics, maize *tan1* mutants have short stature and misoriented cell patterns (23), as do mutants of TAN1-interacting partners *phragmoplast orienting kinesin-1;2* (24). TAN1 is similar to the microtubule binding domain of adenomapolyposis coli (22), a multifunctional protein that promotes proper division orientation in animal cells (25–27). In *Arabidopsis thaliana,* AtTAN1 fused to yellow fluorescent protein (YFP) was the first identified positive marker of the cortical division site, remaining at the site after PPB disassembly (20). AtTAN1-YFP division site recruitment occurs via several independent mechanisms during different cell-cycle stages (21), but AtTAN1 function is still unclear. Because of the mild *tan* mutant phenotype in *A. thaliana* (20), it was impossible to determine whether AtTAN-YFP could rescue the *tan* mutant phenotype.

Fully functional maize TAN1 fused to YFP (TAN1–YFP) and TAN1–YFP lines described below were examined using live-cell imaging to assess TAN1 function. One TAN1–YFP line with the destruction box from CYCLIN1B fused to TAN1–YFP (D-TAN1-13–YFP), showed partial rescue of the *tan1* mutant. D-TAN1-13–YFP in the *tan1* mutant background exhibited significant delays in mitotic progression, but only minor defects in division plane orientation. Analysis of this variant allowed us to assess the relative importance of mitotic delays and phragmoplast guidance to the division site. D-TAN1-13–YFP in the *tan1* mutant background grew to the same size as wild-type, suggesting that compensatory mechanisms could rescue growth impacted by mitotic delays but not a combination of mitotic delays and division plane orientation defects.

Significance

Speculation about the role of division plane orientation in the growth of a plant has hinged on two conflicting ideas. The first idea is that the plant body is specified at the tissue level and cells divide merely to fill in the space, making the orientation of division unimportant to the overall growth. The second idea is that the orientation of the division plane is critical for tissue-level patterning and therefore also impacts growth. This study suggests that misorientation of the division plane together with cell-cycle delays cannot be compensated for. Therefore, division plane orientation is a critical but potentially indirect factor for growth.

Author contributions: P.M. and C.G.R. designed research; P.M. and C.G.R. performed research; A.L., A.S., and C.G.R. contributed new reagents/analytic tools; P.M. and C.G.R. created the figures; A.L. produced the TAN1-YFP construct and sequenced the upstream regulatory region of the *tan1* gene to ensure normal regulatory functions and produced the CFP-TUB construct; P.M. and C.G.R. analyzed data; and P.M. and C.G.R. wrote the paper.

The authors declare no conflict of interest.

This article is a PNAS Direct Submission.

Freely available online through the PNAS open access option.

[1]To whom correspondence should be addressed. Email: carolyn.rasmussen@ucr.edu.

This article contains supporting information online at www.pnas.org/lookup/suppl/doi:10.1073/pnas.1619252114/-/DCSupplemental.

Results and Discussion

Maize *tan1* mutants have short stature and rough textured leaves with disordered cell patterning and shapes (28) (Fig. S1 *A–C*) but did not have cytokinesis defects, such as incomplete cell-wall stubs or multinucleate cells (Fig. S1*E*) (23). Moreover, cells derived from both symmetric and asymmetric divisions were abnormally shaped (Fig. S1*E*), indicating that TAN1 function is required for proper division plane orientation in symmetrically and asymmetrically dividing cells.

Previous studies suggested that *tan1* mutants have division plane defects caused by the inability of phragmoplasts to track back to the division site (29). However, these experiments were conducted with fixed cells: it was not possible to compare the location of the PPB to the final orientation of the completed division. YFP-TUBULIN (30) was crossed into *tan1* mutants to directly test the hypothesis that *tan1* mutants had a phragmoplast guidance defect using time-lapse imaging. Wild-type and *tan1* mutant cells expressing YFP-TUBULIN were imaged from prophase until the end of cytokinesis and compiled into a single time-lapse to compare PPB location to the final division plane (Fig. 1*A*, six other examples in Fig. 1*B*, and Movie S1). In wild-type cells all completed divisions displayed normal division orientation: the new cell wall aligned with the former location of the PPB ($n = 87$). When *tan1* mutant cells were observed 62.5% ($n =$ 30 of 48) of new cell walls returned to the division site previously occupied by the PPB (Fig. 1*C* and Movie S2), whereas 37.5% of new cell walls displayed an aberrant location (Fig. 1 *D* and *E* and Movie S3). These data provide direct evidence that *tan1* mutant cells have defects in division plane orientation because of a phragmoplast guidance defect.

While performing temperature controlled time-lapse imaging (31), we observed that *tan1* mutant cells were delayed in both metaphase (Fig. 2*A*) and telophase (Fig. 2*B*), but not anaphase compared with wild-type siblings (Fig. S2). Time-lapse imaging was performed by taking a *Z*-stack every 5 min and assessing at each time the morphology of the mitotic structure. The start of metaphase was counted from the first time the spindle was observed until the anaphase spindle was observed. This time-point became the first time-point for anaphase. Telophase timing was measured from the first time-point a phragmoplast was observed until the phragmoplast was completely disassembled (31). There was no correlation between metaphase delay and defects in phragmoplast guidance to the division site (Fig. S3*A*), and no correlation between metaphase and telophase delays (Fig. S3*B*). Next, phragmoplast dynamics were analyzed during telophase to determine whether delays in telophase were a result of slower phragmoplast expansion rates in addition to failure to return to the division site. Phragmoplast expansion (Fig. 2*C*) and disassembly (Fig. 2*D*) were slower in *tan1* mutant cells versus wild-type, but there was no correlation between slow phragmoplast expansion and misoriented phragmoplast orientation (Fig. S3*C*) [Kolmogorov–Smirnov (KS) test, $P > 0.1$]. The delays in metaphase and telophase suggest that TAN1 may alter microtubule stability or dynamics in mitotic microtubule arrays. Lack of correlation between mitotic delays and misguided phragmoplast orientation suggest that mitotic progression and proper division plane orientation may be separate.

TAN1 driven by its own promoter was fused to YFP and transformed into maize (32): TAN1–YFP fully rescued the mutant phenotype (Fig. 3*N*) and was observed only in mitotic or late G2 cells. TAN1–YFP localized to the cortical division site in symmetrically (Fig. 3 *A–D*) and asymmetrically (Fig. S4) dividing cells. Low TAN1–YFP fluorescence intensity was often observed during G2 (Fig. 3*I*), suggesting that TAN1–YFP was recruited to the division site after PPB formation. After prophase, TAN1–YFP accumulated at the cortical division site and stayed at the same level until the end of telophase (Fig. 3 *A–D* and *I*). In addition to cortical division site localization, TAN1–YFP faintly colocalized with the metaphase spindle (Fig. 3*B*) (~23% fluorescence intensity compared with TAN1–YFP at the cortical division site, $n = 25$), anaphase spindle (Fig. 3*C*) (~10% fluorescence intensity compared with TAN1–YFP at cortical division site, $n = 6$), and phragmoplast microtubules (Fig. 3*D*) (~15% fluorescence intensity compared with TAN1–YFP at the cortical division site, $n = 21$). Spindle and phragmoplast localization of TAN1–YFP together with in vitro TAN1–microtubule interaction (22) is consistent with the hypothesis that TAN1 directly alters microtubule dynamics in these structures. AtTAN–YFP did not appear to colocalize with the spindle or phragmoplast in *A. thaliana* (20, 21). The faint nucleolar localization of TAN1–YFP (Fig. 3*A*) was similar to that observed in AtTAN–YFP cells (21). TAN1–YFP was crossed into the *tan1* mutant to determine if it rescued the mutant phenotype. A population segregating for *tan1*/+ (Fig. 3*L*), *tan1*/*tan1* (Fig. 3*M*), and the TAN1–YFP transgene (Fig. 3*N*) was assessed for growth by measuring the area of several leaf blades (leaf 7 in Fig. 3*K* and leaves 5 and 8 in Fig. S5).

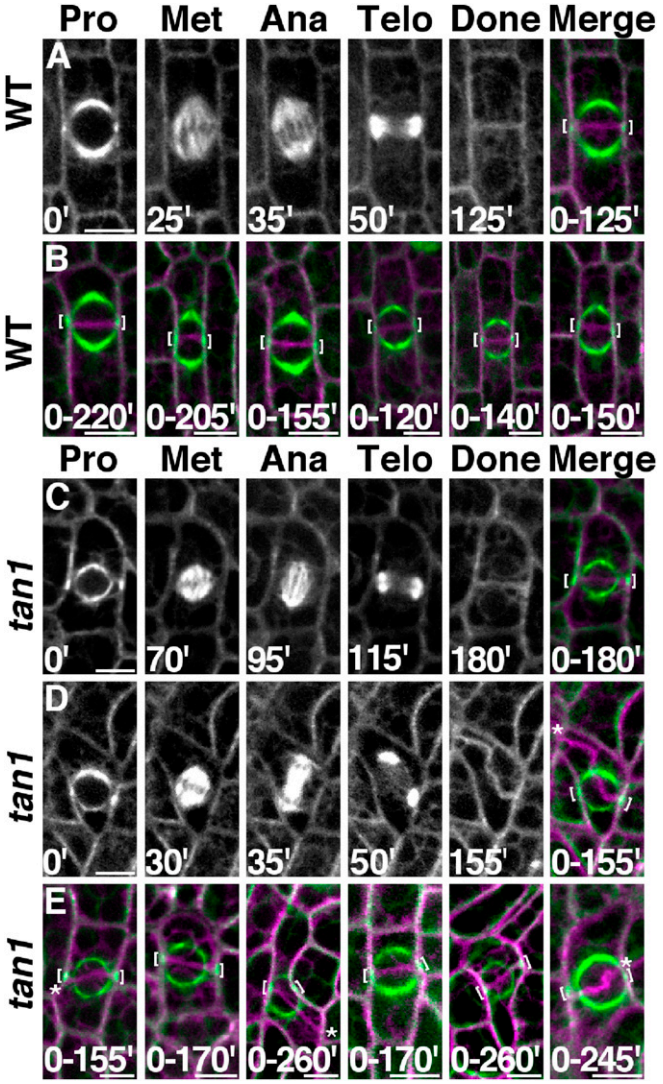

Fig. 1. Time-lapse and division-time quantification. Merged images show before (green) and after (magenta) division. (*A*) Wild-type cell division. (*B*) Six representative wild-type cells. (*C*) Correctly oriented *tan1* cell division. (*D*) Misoriented *tan1* division. (*E*) Six representative *tan1* cells. Brackets mark PPB location. Misplaced cell walls indicated by asterisks. Time (minutes) at the bottom of the image. (Scale bars, 10 μm.)

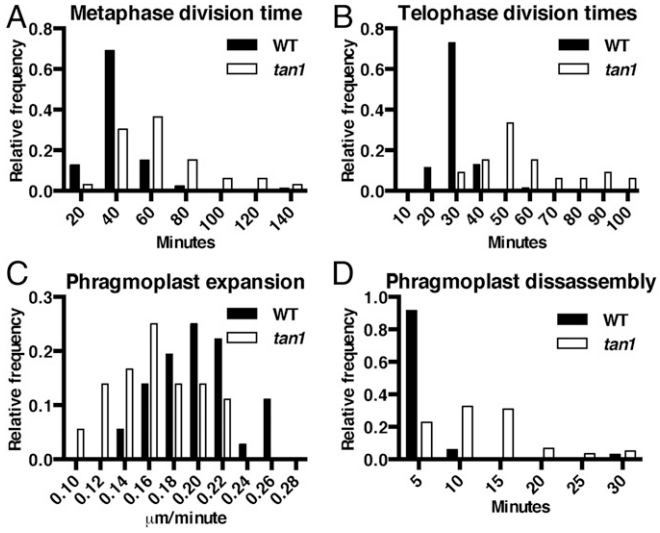

Fig. 2. Histograms of time required to complete mitotic stages of wild-type and *tan1* mutant cells. (*A*) Metaphase times: wild-type (39 min, $n = 87$) and *tan1* (61 min, $n = 33$), KS test $P < 0.0001$. (*B*) Transverse telophase times: wild-type (29 min, $n = 70$) and *tan1* (56 min, $n = 33$), KS test, $P < 0.0001$. (*C*) Phragmoplast expansion rates of wild-type (0.20 ± 0.01 μm/min, $n = 18$ cells) and *tan1* (0.16 ± 0.01 μm/min, $n = 18$ cells, KS test, $P < 0.001$). (*D*) Phragmoplast disassembly times for wild-type (6 min, $n = 70$) and *tan1* (12.5 min, $n = 31$), KS test, $P < 0.0001$.

TAN1–YFP; *tan1*/*tan1* displayed both wild-type growth (Fig. 3*K*) (KS test, $P = 0.16$) and cell-wall patterning similar to wild-type (Fig. 3*N*) ($n = 13$ individual plants), indicating that TAN1–YFP fully rescued the mutant phenotype.

The phragmoplast guidance defect observed in the *tan1* mutant (Fig. 1), together with temporally separate AtTAN recruitment to the division site during both prophase and telophase (21), suggested that TAN1 has a critical function during telophase. We used a TAN1–YFP fusion containing the CYCLIN1B (GRMZM2G034647) destruction box (D-TAN1–YFP) to assess the function of TAN1 after anaphase. Maize CYCLIN1B is degraded in anaphase (33) and *A. thaliana* CYCLIN1B homolog has been used to degrade proteins during anaphase (34, 35). A negative control with a mutated destruction box was also created (mD-TAN1–YFP). Three independently transformed D-TAN1–YFP and mD-TAN1–YFP lines were crossed into lines expressing cyan-fluorescent protein (CFP)–TUBULIN and the *tan1* mutant to assess localization and rescue. mD-TAN1–YFP localized to the division site similar to TAN1–YFP and had similar fluorescent intensities (Fig. S6 *A–F*), indicating that adding a sequence to the N terminus does not alter division site localization or relative fluorescence intensities. All mD-TAN1 lines completely rescued the short stature of the *tan1* mutant and had leaves with the same size quantified through measurement of leaf areas (Fig. S7 *D–F*). D-TAN1–YFP also localized to the division site, but fluorescence signal significantly decreased at the division site as telophase progressed (D-TAN1-13–YFP in Fig. 3 *E–H*, and *J* and D-TAN1-3–YFP and D-TAN1-21–YFP in Fig. S6 *G–J*). Quantification of fluorescence intensities at the division site indicated that D-TAN1–YFP from three independently transformed lines was eliminated in telophase only when the phragmoplast >10 μm and after the majority of transverse divisions were completed (D-TAN1-13–YFP in Fig. 3*J* D-TAN1-3–YFP and D-TAN1-21–YFP in Fig. S6 *H* and *J*). Therefore, the destruction box, although it eventually led to D-TAN1–YFP elimination from the division site, did not eliminate D-TAN1–YFP completely before the majority of cells finished cytokinesis.

One line containing the D-box-TAN1–YFP fusion, D-TAN1–YFP-13 (Fig. 3 *E–H*), had low fluorescent intensity at the division site during all mitotic stages, but had exceptionally low intensity during telophase (quantified in Fig. 3*J*) and had no detectable signal in spindles (Fig. 3 *F* and *G*) or phragmoplasts (Fig. 3*H*). Although all of the mD-TAN1–YFP and two other D-TAN1–YFP transgenes fully rescued the *tan1* mutant division plane defects (mD-TAN1–YFP in Fig. S7 *A–C* and D-TAN1–YFP in Fig. S8 *A* and *B*), D-TAN1-13–YFP *tan1*/*tan1,* had minor division plane defects first observed by cell-wall staining (Fig. 3*O*) and then quantified by time-lapse imaging of D-TAN1-13–YFP *tan1*/*tan1* dividing cells (described below). All three of the D-TAN1 lines completely rescued the growth defect of the *tan1* mutant quantified via multiple leaf area measurements made at 28 d after planting (D-TAN1 lines #3 and #21 in Fig. S8 *C–E*). D-TAN1-13–YFP plant development was additionally compared with wild-type siblings at 1 wk (Fig. S9), 2 wk (Fig. S10), and 3 wk (Fig. S11) after planting.

Two hypotheses could explain the division plane defects in D-TAN1-13–YFP *tan1*/*tan1* line: (*i*) overall low expression of D-TAN1-13–YFP provided insufficient protein to fully rescue the mutant phenotype during all stages; or (*ii*) low levels of D-TAN1-13–YFP during telophase caused the division plane defect observed. If loss of TAN1 exclusively during telophase caused division plane defects, metaphase division times would be the same as wild-type, whereas telophase times would be longer. In contrast, live-cell imaging indicated that both metaphase and telophase times in D-TAN1-13–YFP *tan1*/*tan1* cells were intermediate between wild-type and *tan1* mutants (Fig. 4). During this time-lapse analysis, one aberrant division was observed ($n = 1$ of 106, < 1%) indicating that D-TAN1-13–YFP *tan1*/*tan1* cells have minor defects in division plane orientation (Movie S4). Phragmoplast expansion rates of *tan1* D-TAN1-13 were significantly slower than wild-type, and similar to phragmoplast expansion rates observed in the *tan1* mutant (Fig. S12). Total division time of measured mitotic stages (metaphase, anaphase, telophase) for *tan1* (average 123 min, $n = 33$ from Fig. 2 dataset) are delayed by 66% compared with wild-type (average 74 min, $n = 70$), whereas the D-TAN1-13–YFP *tan1*/*tan1* partial rescue plants (average 94 min, $n = 90$) have 40% of the mitotic delay seen in the *tan1* mutant. Minor division plane orientation defects were observed in D-TAN1-13–YFP *tan1*/*tan1*lines (<1%, $n = 1$ misoriented division of 106 completed divisions) compared with *tan1* mutants (~37%, $n = 48$). This finding suggested that D-TAN1-13–YFP *tan1*/*tan1* represents a partial loss of function mutant because of low expression rather than a telophase-specific defect. In addition, undetectably low D-TAN1–YFP fluorescent intensities at spindles or phragmoplasts together with observed mitotic delays in D-TAN1-13–YFP *tan1*/*tan1* lines is consistent with a role of TAN1 in altering microtubule dynamics at mitotic structures. Therefore, D-TAN1-13–YFP *tan1*/*tan1* represented a partial loss-of-function mutant, where significant mitotic delays were observed but division plane defects were infrequent.

We predicted that the poorly expressed D-TAN1–YFP partial rescue line would have growth defects intermediate to the *tan1* mutant and wild-type siblings because it had intermediate cell-cycle delays. However, D-TAN1-13–YFP *tan1*/*tan1* plants grew as well as wild-type siblings. Growth and development of sibling plants was assessed by taking pictures of plants, measuring shoot and root wet weight, and determining length, area and average width of the leaves (Figs. S9–S13). Completely rescued growth of plants with cell-cycle delays and minor division plane defects suggested that defects in cell-cycle progression and minor division plane orientation were corrected, potentially by expansion or by another compensatory mechanism (36). We measured cell area in the proliferative division zone of the maize blade, but no significant difference was observed between sibling wild-type and

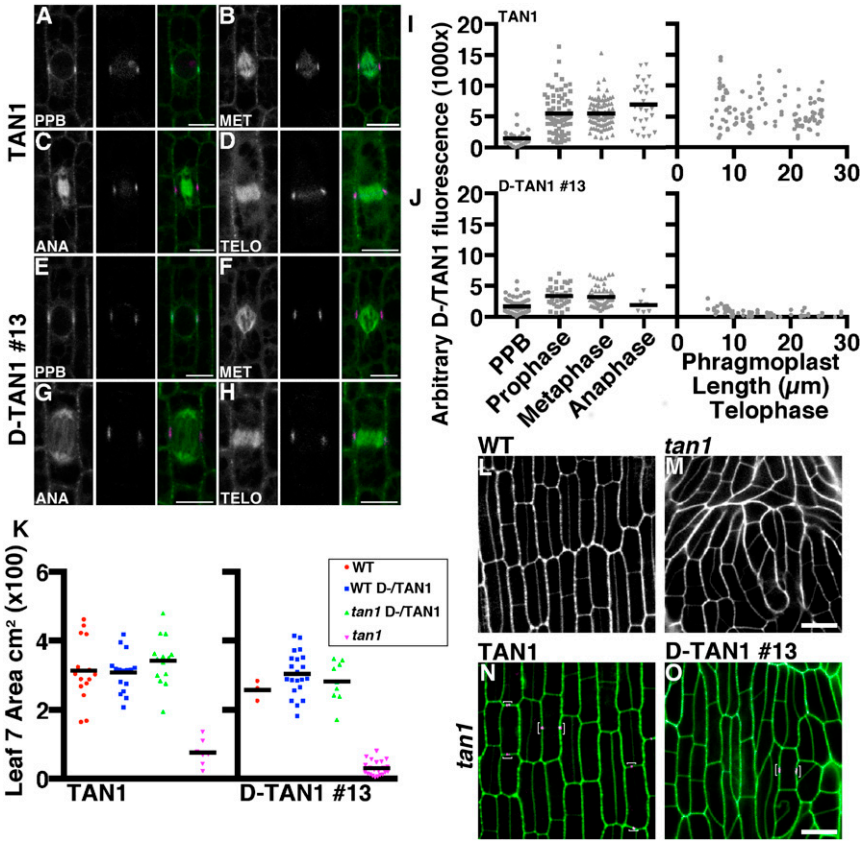

Fig. 3. Localization and rescue of TAN1–YFP and D-TAN1-13–YFP during mitosis and cytokinesis. TAN1–YFP (magenta) localization during prophase (*A*), metaphase (*B*), anaphase (*C*), and telophase (*D*) indicated by CFP–TUBULIN (green). Channels are separated CFP–TUBULIN followed by TAN1–YFP and then merged. D-TAN1-13–YFP (magenta) localization during prophase (*E*), metaphase (*F*), anaphase (*G*), and telophase (*H*) indicated by CFP–TUBULIN (green). Channels are separated CFP–TUBULIN followed by TAN1–YFP and then merged. Arbitrary fluorescence intensities measured at the division site for TAN1–YFP (*I*) and D-TAN1 (*J*) using identical imaging conditions. (*K*) Leaf 7 area measurements of wild-type and *tan1* segregating with TAN1–YFP and D-TAN1-13–YFP. Leaf areas between wild-type and *tan1* TAN1–YFP are not statistically different (KS test, $P = 0.1994$) and are not different between wild-type and *tan1* D-TAN1-13–YFP (KS test, $P = 0.7091$). (*L*) Wild-type and (*M*) *tan1* epidermal cells stained with propidium iodide (green). (*N*) TAN1–YFP (magenta) expressed in *tan1* mutant background stained with propidium iodide (green). (*O*) D-TAN1-13–YFP (magenta) in the *tan1* mutant background stained with propidium iodide (green). (Scale bars, 10 μm.)

D-TAN1-13–YFP cells, suggesting either that another compensatory mechanism is used or that the cells compensate by expansion in another part of the leaf (Fig. S14). In some cases, cell-cycle delays do not noticeably alter overall plant (37) or animal (38) growth, but other cell-cycle delays alter embryonic or root patterning in *A. thaliana* (39, 40). More severe cell-cycle delays using overexpression of cyclin-dependent kinase inhibitor, ICK1, demonstrated that cell expansion could partially compensate for mitotic delays. However, slow cell-cycle progression still led to abnormal growth and development (41).

The small stature of *tan1* mutants suggested that division orientation and proper cell-cycle timing are important aspects of plant growth. The simplest interpretation of the small stature of the *tan1*mutant compared with the normal growth of the partially rescued D-TAN-13–YFP *tan1* line is that proper division orientation is directly required for plant growth. Alternatively, the short stature of the *tan1* mutant might indicate slowed growth in response to altered cell shape. Indeed, cell shape and corresponding mechanical constraints influence growth, even in the absence of cell division (36). Another interpretation is that altered cell-wall placement causes unexpected mechanical strain, which then activates a biochemical response, such as the cell-wall integrity pathway, to slow growth (42). These hypotheses are not mutually exclusive.

Most division plane orientation mutants likely also have mitotic delays, although this phenotype has only rarely been assessed (24, 43). In addition, many symmetric division plane orientation mutants have defects in both interphase and mitotic microtubule dynamics, making it impossible to address mitotic and interphase function independently (10–12, 43–47). There are a few mutants

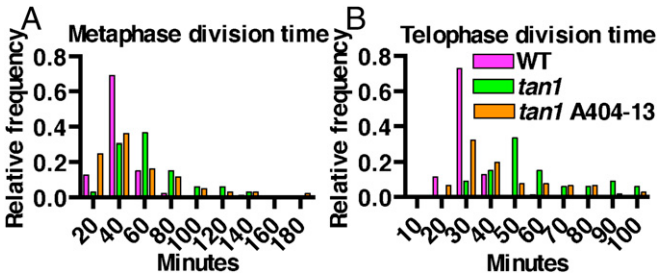

Fig. 4. Partial rescue during metaphase and telophase of D-TAN1-13–YFP in the *tan1* mutant background. Data for wild-type and *tan1* is the same as presented in Fig. 2 *A* and *B*, graphed alongside the *tan1* D-TAN1-13 data for direct comparison. (*A*) Metaphase division time for *tan1* D-TAN1-13–YFP cells (51 ± 6.4 min, 95% CI, $n = 106$). Metaphase times are significantly different from wild-type (KS test, $P = 0.0027$) and from *tan1* (KS test, $P = 0.0002$). (*B*) Telophase times (36.3 ± 3 min 95% CI $n = 90$) for transverse cell divisions. Telophase times are significantly different from wild-type (KS test, $P < 0.0001$) and from *tan1* (KS test, $P = 0.0007$).

that represent intriguing exceptions to highly pleiotropic mutants. One example is the *sabre* mutant, which has misplaced PPBs rather than defective or absent PPBs, leading to defects in establishing the proper division plane orientation in *A. thaliana* (48). Another example is a quintupule *myosinVIII* mutant generated in *Physcomitrella patens.* These mutants display division plane defects in cells that undergo PPB-independent divisions (49). The MYOSINVIII protein promotes proper phragmoplast guidance while localizing to the spindle, phragmoplast midzone, and the division site. The proposed model is that MYOSINVIII moves along actin filaments to properly translocate the microtubules in the phragmoplast toward the division site (50). TAN1 is only present during mitosis, so mutant analysis provides understanding of mitotic specific division plane orientation and cell-cycle progression. This study highlights the importance of correct division plane orientation and timely cell-cycle progression to maintain proper growth.

Materials and Methods

Plants were grown in standard greenhouse conditions. Transgenic maize lines were generated as part of the maize cell genomics project (maize.jcvi.org/cellgenomics/index.php), including YFP variant Citrine fused to α-TUBULIN (YFP–TUBULIN, GRMZM2G153292) and cyan-fluorescent protein fused to β-TUBULIN (CFP–TUBULIN, GRMZM2G164696) (30). A.L. created the TANGLED1 transgene through translational fusion with the YFP variant Citrine (TAN1–YFP, GRMZM2G039113) described in *SI Materials and Methods*. Construction of D-TAN1–YFP and mD-TAN1–YFP fused wild-type or mutated CYCLIN1B coding sequence from maize GRMZM2G034647 to the N-terminal end of TAN1 is described in *SI Materials and Methods*.

All time-lapse and quantitative fluorescent imaging was done using a custom-built spinning disk system (Solamere Technology) described in *SI Materials and Methods*. Time-lapse imaging experiments were performed using standardized imaging conditions. Four-week-old plants were used and leaves were removed until the ligule height was <2 mm. Adaxial symmetrically dividing blade samples were mounted in water, surrounded by vacuum grease on a coverslip, and loaded with another coverslip placed carefully on top of the sample into a Rose chamber (51) and held at constant temperature (21 °C) (31). *Z*-stacks of cells in late prophase were taken every 5 min for up to 6 h. Only cells that completed a division from prophase until the new cell wall was formed were used to analyze the timing of cell-cycle stages to ensure that the cells used in the analysis were not damaged during sample preparation. Morphology of mitotic structures labeled with YFP–TUBULIN was assessed to infer mitotic stage. Metaphase timing included first time the spindle was observed until the anaphase spindle was observed. This time-point became the first time-point for anaphase. Anaphase spindles rapidly transitioned to phragmoplasts in telophase. Telophase timing was measured from the first time-point a phragmoplast was observed until the phragmoplast was completely disassembled (31).

For quantification of fluorescence intensities, micrographs were taken of TAN1–YFP, mD-TAN1–YFP, and D-TAN1–YFP lines using standardized imaging conditions. Plants coexpressing CFP–TUBULIN were used to identify each stage of mitosis. *Z*-stacks were transformed into maximum projections in ImageJ or FIJI (fiji.sc/) using two or more *Z* slices. Sample movement was corrected using the StackReg Plugin in FIJI. Micrographs for Fig. 3 *A–H* and Fig. S6 *C, E, G,* and *I* were taken with a point scanning confocal microscope (SP5, Leica) with HyD detector with Argon 514-nm laser emission 510–601 nm for each mD- or D-TAN1–YFP and 458 with emission 505–510 nm for CFP–TUBULIN using a 40× NA 1.1 water objective.

See Table S1 for primers used in this study.

ACKNOWLEDGMENTS. We thank Professors Laurie Smith (University of California, San Diego) for initial TAN1–YFP crosses, Thomas Eulgem (University of California, Riverside), J. Gatlin (University of Wyoming), Zhaojie Zhang (University of Wyoming), and Dr. David Carter (University of California, Riverside) for microscope use. We also thank the University of Wyoming Agriculture Experiment Station and University of California, Riverside Agricultural Operations for greenhouse and field space; the Plant Transformation Facility (Dr. Kan Wang and Bronwyn Frame, Iowa State University) for maize transformation; and Leslie Z. Aranda, McKenzie R. Pickle, Victoria H. Morris, Leticia Meza, and Lindy A. Allsman for help with measuring leaf areas. A.S. is appreciative of the collaborative interactions with the maize cell genomics group. A.S. provided field space, funds, and reagents to create and transform mD-TAN1-YFP and D-TAN1-YFP into maize and supported initial analysis and imaging of the lines. An IDeA-National Institute of General Medical Sciences-NIH Grant P30-GM103398 (to the University of Wyoming) supplemented use of scanning electron microscope. This work was supported by National Science Foundation Grants DBI-0501862 and MCB-1027445 (to A.S.) and National Science Foundation Grants NSF-MCB-1505848, NSF-MCB-1244202, and US Department of Agriculture Grant USDA-NIFA-CA-R-BPS-5108-H (to C.G.R.).

1. Kaplan DR, Hagemann W (1991) The relationship of cell and organism in vascular plants. *Bioscience* 41(10):693–703.
2. Beemster GTS, Fiorani F, Inzé D (2003) Cell cycle: The key to plant growth control? *Trends Plant Sci* 8(4):154–158.
3. Rasmussen CG, Wright AJ, Müller S (2013) The role of the cytoskeleton and associated proteins in determination of the plant cell division plane. *Plant J* 75(2):258–269.
4. Murata T, et al. (2013) Mechanism of microtubule array expansion in the cytokinetic phragmoplast. *Nat Commun* 4:1967.
5. Jürgens G (2005) Cytokinesis in higher plants. *Annu Rev Plant Biol* 56:281–299.
6. Van Damme D (2009) Division plane determination during plant somatic cytokinesis. *Curr Opin Plant Biol* 12(6):745–751.
7. Chan J, Calder G, Fox S, Lloyd C (2005) Localization of the microtubule end binding protein EB1 reveals alternative pathways of spindle development in *Arabidopsis* suspension cells. *Plant Cell* 17(6):1737–1748.
8. Ambrose JC, Cyr R (2008) Mitotic spindle organization by the preprophase band. *Mol Plant* 1(6):950–960.
9. Buschmann H, et al. (2006) Microtubule-associated AIR9 recognizes the cortical division site at preprophase and cell-plate insertion. *Curr Biol* 16(19):1938–1943.
10. Camilleri C, et al. (2002) The *Arabidopsis* TONNEAU2 gene encodes a putative novel protein phosphatase 2A regulatory subunit essential for the control of the cortical cytoskeleton. *Plant Cell* 14(4):833–845.
11. Azimzadeh J, et al. (2008) *Arabidopsis* TONNEAU1 proteins are essential for preprophase band formation and interact with centrin. *Plant Cell* 20(8):2146–2159.
12. Wright AJ, Gallagher K, Smith LG (2009) discordia1 and alternative discordia1 function redundantly at the cortical division site to promote preprophase band formation and orient division planes in maize. *Plant Cell* 21(1):234–247.
13. De Smet I, Beeckman T (2011) Asymmetric cell division in land plants and algae: The driving force for differentiation. *Nat Rev Mol Cell Biol* 12(3):177–188.
14. Kajala K, et al. (2014) Omics and modelling approaches for understanding regulation of asymmetric cell divisions in *Arabidopsis* and other angiosperm plants. *Ann Bot (Lond)* 113(7):1083–1105.
15. Facette MR, Smith LG (2012) Division polarity in developing stomata. *Curr Opin Plant Biol* 15(6):585–592.
16. Fisher AP, Sozzani R (2016) Uncovering the networks involved in stem cell maintenance and asymmetric cell division in the *Arabidopsis* root. *Curr Opin Plant Biol* 29: 38–43.
17. Shao W, Dong J (2016) Polarity in plant asymmetric cell division: Division orientation and cell fate differentiation. *Dev Biol* 419(1):121–131.
18. van Dop M, Liao C-Y, Weijers D (2015) Control of oriented cell division in the *Arabidopsis* embryo. *Curr Opin Plant Biol* 23:25–30.
19. Han S-K, Torii KU (2016) Lineage-specific stem cells, signals and asymmetries during stomatal development. *Development* 143(8):1259–1270.
20. Walker KL, Müller S, Moss D, Ehrhardt DW, Smith LG (2007) *Arabidopsis* TANGLED identifies the division plane throughout mitosis and cytokinesis. *Curr Biol* 17(21):1827–1836.
21. Rasmussen CG, Sun B, Smith LG (2011) Tangled localization at the cortical division site of plant cells occurs by several mechanisms. *J Cell Sci* 124(Pt 2):270–279.
22. Smith LG, Gerttula SM, Han S, Levy J (2001) Tangled1: A microtubule binding protein required for the spatial control of cytokinesis in maize. *J Cell Biol* 152(1):231–236.
23. Smith LG, Hake S, Sylvester AW (1996) The tangled-1 mutation alters cell division orientations throughout maize leaf development without altering leaf shape. *Development* 122(2):481–489.
24. Lipka E, et al. (2014) The phragmoplast-orienting kinesin-12 class proteins translate the positional information of the preprophase band to establish the cortical division zone in *Arabidopsis thaliana*. *Plant Cell* 26(6):2617–2632.
25. Feng Y, et al. (2013) Sox9 induction, ectopic Paneth cells, and mitotic spindle axis defects in mouse colon adenomatous epithelium arising from conditional biallelic Apc inactivation. *Am J Pathol* 183(2):493–503.
26. Yamashita YM, Jones DL, Fuller MT (2003) Orientation of asymmetric stem cell division by the APC tumor suppressor and centrosome. *Science* 301(5639):1547–1550.
27. Poulton JS, Mu FW, Roberts DM, Peifer M (2013) APC2 and Axin promote mitotic fidelity by facilitating centrosome separation and cytoskeletal regulation. *Development* 140(20): 4226–4236.
28. Mitkovski M, Sylvester AW (2003) Analysis of cell patterns in developing maize leaves: Dark-induced cell expansion restores normal division orientation in the mutant tangled. *Int J Plant Sci* 164(1):113–124.
29. Cleary AL, Smith LG (1998) The *Tangled1* gene is required for spatial control of cytoskeletal arrays associated with cell division during maize leaf development. *Plant Cell* 10(11):1875–1888.
30. Mohanty A, et al. (2009) Advancing cell biology and functional genomics in maize using fluorescent protein-tagged lines. *Plant Physiol* 149(2):601–605.
31. Rasmussen CG (2016) Using live-cell markers in maize to analyze cell division orientation and timing. *Plant Cell Division*, ed Caillaud M-C (Springer, New York), pp 209–225.

32. Wu Q, Luo A, Zadrozny T, Sylvester A, Jackson D (2013) Fluorescent protein marker lines in maize: Generation and applications. *Int J Dev Biol* 57(6-8):535–543.
33. Mews M, et al. (1997) Mitotic cyclin distribution during maize cell division: Implications for the sequence diversity and function of cyclins in plants. *Protoplasma* 200(3):128–145.
34. Krupnova T, et al. (2009) Microtubule-associated kinase-like protein RUNKEL needed [corrected] for cell plate expansion in *Arabidopsis* cytokinesis. *Curr Biol* 19(6):518–523, erratum in Curr Biol 2009, 19(6):536.
35. Van Damme D, et al. (2011) *Arabidopsis* α Aurora kinases function in formative cell division plane orientation. *Plant Cell* 23(11):4013–4024.
36. Bassel GW, et al. (2014) Mechanical constraints imposed by 3D cellular geometry and arrangement modulate growth patterns in the *Arabidopsis* embryo. *Proc Natl Acad Sci USA* 111(23):8685–8690.
37. Hemerly A, et al. (1995) Dominant negative mutants of the Cdc2 kinase uncouple cell division from iterative plant development. *EMBO J* 14(16):3925–3936.
38. Neufeld TP, de la Cruz AF, Johnston LA, Edgar BA (1998) Coordination of growth and cell division in the *Drosophila* wing. *Cell* 93(7):1183–1193.
39. Jenik PD, Jurkuta RE, Barton MK (2005) Interactions between the cell cycle and embryonic patterning in *Arabidopsis* uncovered by a mutation in DNA polymerase epsilon. *Plant Cell* 17(12):3362–3377.
40. Sozzani R, et al. (2010) Spatiotemporal regulation of cell-cycle genes by SHORTROOT links patterning and growth. *Nature* 466(7302):128–132.
41. Wang H, Zhou Y, Gilmer S, Whitwill S, Fowke LC (2000) Expression of the plant cyclin-dependent kinase inhibitor ICK1 affects cell division, plant growth and morphology. *Plant J* 24(5):613–623.
42. Voxeur A, Höfte H (2016) Cell wall integrity signaling in plants: "To grow or not to grow that's the question". *Glycobiology* 26(9):950–960.
43. Kawamura E, et al. (2006) MICROTUBULE ORGANIZATION 1 regulates structure and function of microtubule arrays during mitosis and cytokinesis in the *Arabidopsis* root. *Plant Physiol* 140(1):102–114.
44. Spinner L, et al. (2010) The function of TONNEAU1 in moss reveals ancient mechanisms of division plane specification and cell elongation in land plants. *Development* 137(16):2733–2742.
45. Komaki S, et al. (2010) Nuclear-localized subtype of end-binding 1 protein regulates spindle organization in *Arabidopsis*. *J Cell Sci* 123(Pt 3):451–459.
46. Zhang Y, Iakovidis M, Costa S (2016) Control of patterns of symmetric cell division in the epidermal and cortical tissues of the *Arabidopsis* root. *Development* 143(6): 978–982.
47. Spinner L, et al. (2013) A protein phosphatase 2A complex spatially controls plant cell division. *Nat Commun* 4:1863.
48. Pietra S, et al. (2013) *Arabidopsis* SABRE and CLASP interact to stabilize cell division plane orientation and planar polarity. *Nat Commun* 4:2779.
49. Wu SZ, Ritchie JA, Pan AH, Quatrano RS, Bezanilla M (2011) Myosin VIII regulates protonemal patterning and developmental timing in the moss *Physcomitrella patens*. *Mol Plant* 4(5):909–921.
50. Wu S-Z, Bezanilla M (2014) Myosin VIII associates with microtubule ends and together with actin plays a role in guiding plant cell division. *eLife* 3:e03498.
51. Wadsworth P (2012) Using cultured mammalian cells to study mitosis. *Cold Spring Harb Protoc* 2012(2):205–212.
52. Gao S, et al. (2008) Development of a seed DNA-based genotyping system for marker-assisted selection in maize. *Mol Breed* 22(3):477–494.
53. Sambrook J, Russell DW (2001) Molecular Cloning: A Laboratory Manual (Cold Spring Harbor Laboratory Press, Cold Spring Harbor, NY), 3rd Ed.
54. Mohanty A, Yang Y, Luo A, Sylvester AW, Jackson D (2009) Methods for generation and analysis of fluorescent protein-tagged maize lines. *Methods Mol Biol* 526: 71–89.
55. Hellens R, Mullineaux P, Klee H (2000) Technical Focus: A guide to Agrobacterium binary Ti vectors. *Trends Plant Sci* 5(10):446–451.